Article

Balance of Forces in Self-Assembled Monolayers

Jianzhi Gao, Fangsen Li,[†] and Quanmin Guo*

School of Physics and Astronomy, University of Birmingham, Birmingham, B15 2TT, United Kingdom

ABSTRACT: Self-assembly represents a typical example of bottom-up nanotechnology where the formation of macroscopic structures is driven by forces operating at the molecular level. Under situations where several forces of comparable strength are competing with one another, the stable structure achieved depends on the fine balance of all the forces. A good example is the formation of self-assembled monolayers (SAMs) of non-branched alkanethiol molecules, $CH_3-(CH_2)_n-SH$, on the surface of gold, where the interaction between the S headgroup and the gold substrate competes with the force acting between the alkane tails. Here we demonstrate that, if the tail is short, $n \leq 2$, the S-Au interaction dictates the structure of the SAM. As the tail becomes longer than $n = 2$, the enhanced tail-tail interaction is able to displace the S headgroup. Our finding highlights the importance of the "weak" van der Waals interaction for molecular assembly even in the presence of chemical bonding.
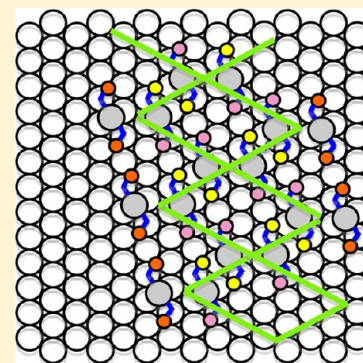
INTRODUCTION

A self-assembled single molecular layer covering a metal or semiconductor substrate has a number of important functions. It can serve as an effective barrier against corrosion and oxidation as well as a buffer layer for tuning the surface chemical properties or a bridging layer for improving biocompatibility.[1] Among all the self-assembled monolayers (SAMs) known so far, alkylthiolate $(CH_3-(CH_2)_n-S)$ layers on gold have attracted the most attention because of the rich chemistry at the thiolate-Au interface.[1−35] Our understanding of the alkylthiolate-Au system has evolved through several important stages. Initially, an alkylthiolate $(CH_3-(CH_2)_n-S)$ species was proposed to bond directly to a perfect Au(111) surface,[1,3,22] and theoretical calculations indicated that the S headgroup is located on either the 3-fold hollow site or the 2-fold bridge site for the frequently observed $(\sqrt{3} \times \sqrt{3})$-R30° structure[29] and its $(3 \times 2\sqrt{3})$-rect./c(4 × 2) variations.[12,30] A photoelectron diffraction study[31] and an independent study employing normal incidence X-ray standing waves (NIXSW),[32] on the other hand, showed that S is located directly above a Au atom. This discrepancy has been partly resolved with the incorporation of Au adatoms.[4,21,36−38] In particular, the discovery of Au-adatom-dithiolate (AAD) on Au(111) in low temperature STM imaging[4] has sparked a new wave of research activities aimed at resolving the interfacial structure of this system.[39−51] Recent high-resolution scanning tunneling microscopy (STM) imaging performed on methylthiolate (MT) and ethylthiolate (ET) monolayers shows that the full monolayers of both MT and ET adopt a (3 × 4) structure[46] at room temperature (RT) on Au(111). Contrary to the established view for over 30 years, the new experimental evidence[46] demonstrates that the $(3 \times 2\sqrt{3})$-rect./c(4 × 2) and $(\sqrt{3} \times \sqrt{3})$-R30° structures do not exist for MT and ET monolayers. A key question to be answered is: what is the connection between the (3 × 4) phase observed for MT and ET monolayers and the $(3 \times 2\sqrt{3})$-rect./c(4 × 2) phase for monolayers of the longer alkanethiols including butanethiol? In order to answer this question, we conducted a detailed structural analysis of the PT monolayer using high-resolution scanning tunneling microscopy (STM). We find that the PT monolayer also favors the (3 × 4) structure. However, the interaction between the propyl chains is strong enough to hinder the formation of large (3 × 4) domains. Two new structural phases have also been identified, and the new findings help us to explain how the stable (3 × 4) phase for MT, ET, and PT monolayers suddenly switches to $(3 \times 2\sqrt{3})$-rect./c(4 × 2) for the butylthiolate monolayer. We propose a unified model for the thiolate-Au interface by recognizing the important role played by nonspecific interactions between the alkane chains. Our results can explain why many previous theoretical attempts failed to predict the correct structure when the interaction between the alkane chains was either completely ignored or oversimplified by considering just a single methyl group.

EXPERIMENTAL SECTION

We conducted experiments in an ultrahigh vacuum (UHV) chamber with a base pressure of 2×10^{-10} mbar using an Omicron variable temperature STM (VT-STM). The gold sample is a (111)-oriented Au film deposited on a highly oriented graphite substrate. The Au film is cleaned using cycles of Ar+ ion sputtering and thermal annealing. The propylthiolate monolayer was prepared by exposing the gold sample to ~10^{-5} mbar of dipropyl-disulfide (DPDS) vapor at room temperature (RT) until saturation coverage was reached. STM imaging was performed at RT using electrochemically etched tungsten tips. The molecular coverage is obtained by finding

the density of the thiolate on the surface, and then, this is normalized with the density of surface gold atoms.

■ RESULTS AND DISCUSSION

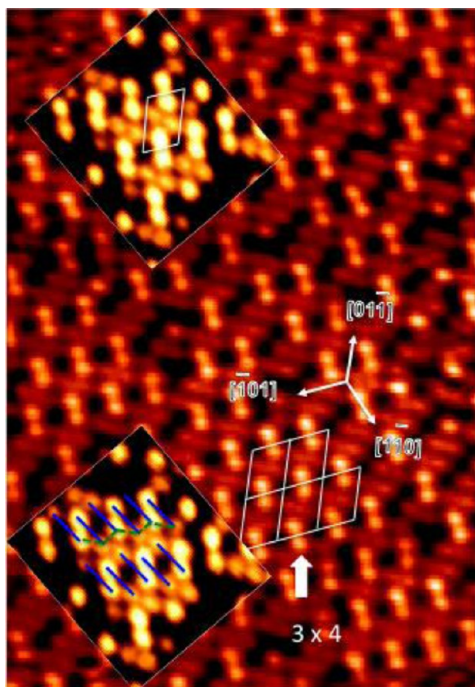Figure 1 shows an STM image of a PT monolayer formed on Au(111) following an exposure to dipropyl-disulfide (DPDS) at

Figure 1. STM image, 11 nm × 15 nm, obtained using a 2.0 V sample bias and 0.3 nA tunneling current from Au(111) with ~1/3 ML of propylthiolate. A local 3 × 4 mesh is illustrated. With high resolution, inset at the upper left corner, it can be seen that within each unit cell there are four spots corresponding to four propyl chains: two bright (taller) spots and two less bright (shorter) ones. The inset at the lower left corner shows the zig-zag rows of AAD units which are highlighted with blue bars.

a pressure of 1×10^{-5} mbar for 1 h. This exposure ensures that the surface reaches a saturation molecular coverage. Following the earlier analysis of MT and ET monolayers,[19,46,51] the bright protrusions in the image are assigned to the CH_3 groups of the propyl chains. By comparing with STM images from MT and ET monolayers,[19,46,51] we can easily identify the presence of the 3 × 4 phase in Figure 1. The inset near the upper left corner of Figure 1 shows a high-resolution image of the 3 × 4 phase with a unit cell illustrated. The 3 × 4 unit cell has the same size as that of a $(3 \times 2\sqrt{3})$-rect. unit cell. The presence of four propyl chains, two of them appearing taller than the other two, inside the unit cell confirms that the coverage is 1/3 monolayer. The inset in the lower left corner of Figure 1 is used to illustrate the zig-zag rows of Au-adatom-dipropylthiolate (AAD), with the blue-colored bars indicating the individual AAD units. There is an obvious difference between the PT monolayer and the MT and ET monolayers. For both MT and ET monolayers, the 3 × 4 phase exists in large domains with linear dimensions up to ~100 nm. In contrast, the 3 × 4 domains are much smaller for the PT monolayer. The rather small size of the 3 × 4 domains is not due to different experimental conditions. It is an intrinsic feature of the PT monolayer as will be discussed later.

Before we discuss the detailed features of the PT monolayer, we would like to make a comparison of STM images from MT, ET, and PT monolayers. Parts a−d of Figure 2 show STM images from the 3 × 4 phase of these three short chain alkylthiolate monolayers. On the basis of what is known for the methyl- and ethylthiolate monolayers,[19,46,51] a structural model for the 3 × 4 phase of the PT monolayer is shown in Figure 2e.

For MT, the Au adatom as well as the methyl groups appear as protrusions in STM images.[19,46,51] Hence, each Au-adatom-dimethylthiolate appears as three protrusions. Two adjacent AAD units appear to join together, forming an AAD "dimer", although there is no real bonding between the two AAD within the dimer. Here the term "dimer" is used merely to reflect the superficial grouping of two AAD units, as shown in STM images. No such obvious grouping is seen for ethyl- and propyl-thiolate monolayers, but we will keep using the term "dimer" for the ease of discussion. In Figure 2a−d, a pair of white bars in each image indicates an AAD dimer. The AAD dimer has previously been referred to as tetramers[24] because the methyl groups appear in groups of four.

For ET and PT monolayers, the methyl group at the end of the alkyl chain becomes further away from the Au(111) substrate due to the increased length of the alkane chain, i.e., closer to the STM tip than the Au adatom. Under normal imaging conditions, the Au adatom is invisible in STM images, so each AAD shows up as two bright spots. In Figure 2a, four circles are drawn into the image to illustrate the locations of the methyl groups inside the unit cell. With the help of these four circles, one can see that the internal structure of the unit cell for a MT layer is essentially the same as that for both ET and PT monolayers. According to Figure 2e, the four propyl chains inside each unit cell are not in the same environment. Two chains labeled as "raised CH_3" in the figure (light gray in color) are sandwiched between two AAD units, and due to steric interaction, these two chains are expected to be standing more vertical than the other two (black color). Therefore, each AAD contributes two protrusions with different brightness (heights) in STM images.

The 3 × 4 phase can also be viewed as consisting of zig-zag AAD rows, as shown with the help of the dotted zig-zag lines in Figure 2e. Within each zig-zag row, electrostatic attraction between negatively charged S and the positively charged Au adatom is expected to play a dominant role in keeping the row stable. An interesting observation is that neighboring (3 × 4) domains are connected with domain walls of a regular pattern, so order is preserved at distances longer than the domain size. Figure 3 shows an STM image with 3 × 4 unit cells superimposed. Each boundary consists of a single row of AAD. On either side of this boundary row, there is a normal 3 × 4 domain. In terms of the zig-zag row description, the zig-zag sequence of the AAD is modified by the presence of the boundary. The existence of the boundaries makes the overall coverage slightly less than 1/3 ML. The global coverage for the monolayer shown in Figure 3 is ~0.325 ML. The 3 × 4 domains, as shown in Figure 3, are either two unit cells or three unit cells wide. The rather strong resistance of the monolayer against the formation of large two-dimensional 3 × 4 domains is a key feature that makes the PT monolayer different from the MT and ET monolayers. A possible explanation is that the 3 × 4 domain is strained, and the strain increases with the chain length. Therefore, regular domain boundaries are formed within the PT monolayer in order to relieve the excessive strain.
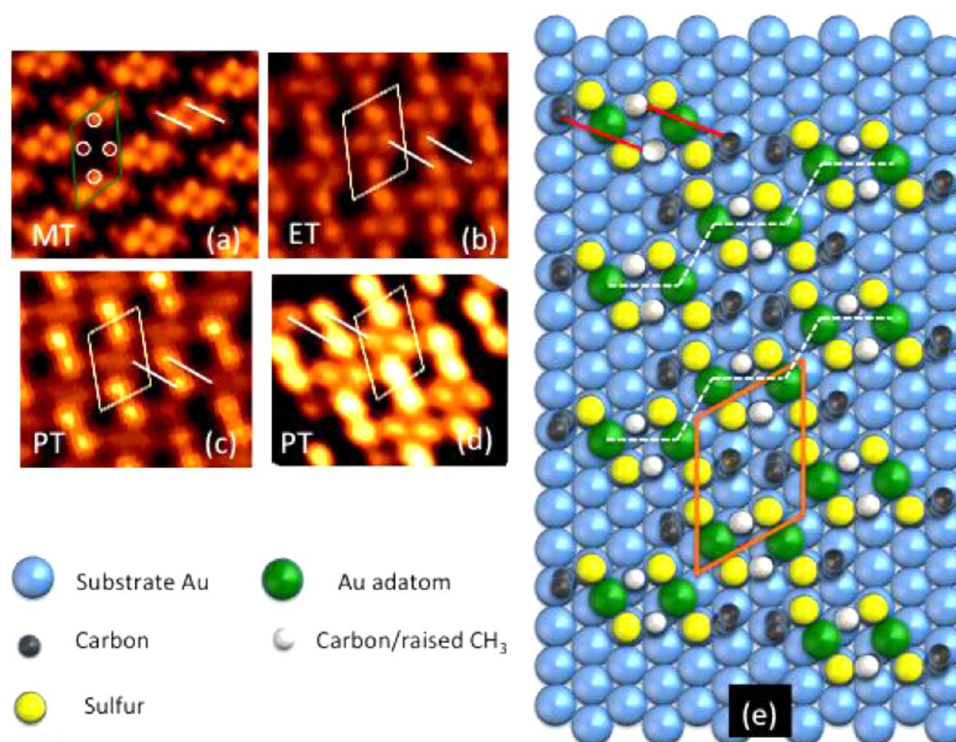
Figure 2. (a–d) STM images from the 3 × 4 phase of methylthiolate (a), ethylthiolate (b), and propylthiolate (c)/(d) monolayers. The white bars in each image are used to highlight the Au-adatom-dithiolate unit. In part a, circles are used to highlight the locations of the methyl groups inside the unit cell. (e) Ball model of the propylthiolate monolayer on Au(111). Dotted white lines indicate the zig-zag arrangement of the AAD rows. Two red bars near the top left corner highlight two AAD units that constitute a "dimer". Partly adapted from ref 52.
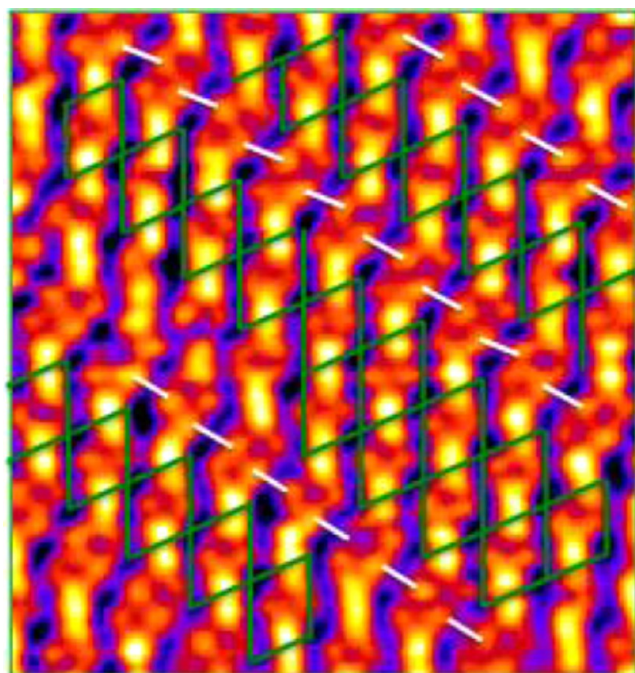

Figure 3. STM image of a propylthiolate layer showing the narrow 3 × 4 domains separated by straight domain boundaries. Solid white bars mark the AAD units forming the boundary.

On the basis of findings from STM imaging, we can conclude that the interfacial bonding between AAD and the Au(111) substrate favors the formation of the 3 × 4 phase at 1/3 ML coverage. Moving from MT to ET, there is hardly any change in the structure of the monolayers despite the doubling of the alkane chain length. As discussed previously, the formation of the 3 × 4 phase is due to the compression of surface AAD units as the coverage approaches 1/3 ML.[51] Thus, as one moves from MT to PT, the increasing length of the alkane chain is expected to play a more and more significant role in responding to such a compression.

An important feature of the 3 × 4 phase is that the distance between the alkane chains is not uniform. For example, the distance between two neighboring tall propyl chains measured from STM images is 0.35 nm. The distance between the short and tall chain within a single AAD is 0.7 nm. For thiolate with longer alkane chains, the van der Waals interaction tends to force the chains into a more regular spacing. Ball models in Figure 4 demonstrate how the 3 × 4 phase could be changed into the $(3 \times 2\sqrt{3})$-rect./c(4 × 2) phase without altering the coverage. The upper part of Figure 4 shows two zig-zag rows of AAD in the 3 × 4 phase. By keeping the top row fixed and translating the lower row along one of the close-packed directions of Au to its new location indicated by the dashed blue line, the 3 × 4 phase is transformed into the $(3 \times 2\sqrt{3})$-rect./c(4 × 2) phase shown at the lower part of the figure. A *cis–trans* isomerization of all AAD units has been introduced at the same time to keep the alkane chains as equally spaced as possible. All non-branched alkylthiolate monolayers with more than three carbons in the chain form the $(3 \times 2\sqrt{3})$-rect./c(4 × 2) phase at 1/3 ML.[1,3] The change from 3 × 4 to $(3 \times 2\sqrt{3})$-rect./c(4 × 2) occurs when moving from PT to butylthiolate (BT). Therefore, the addition of one extra CH_2 unit is enough to enhance the van der Waals interaction to a level to tip the balance toward the $(3 \times 2\sqrt{3})$-rect./c(4 × 2) phase.
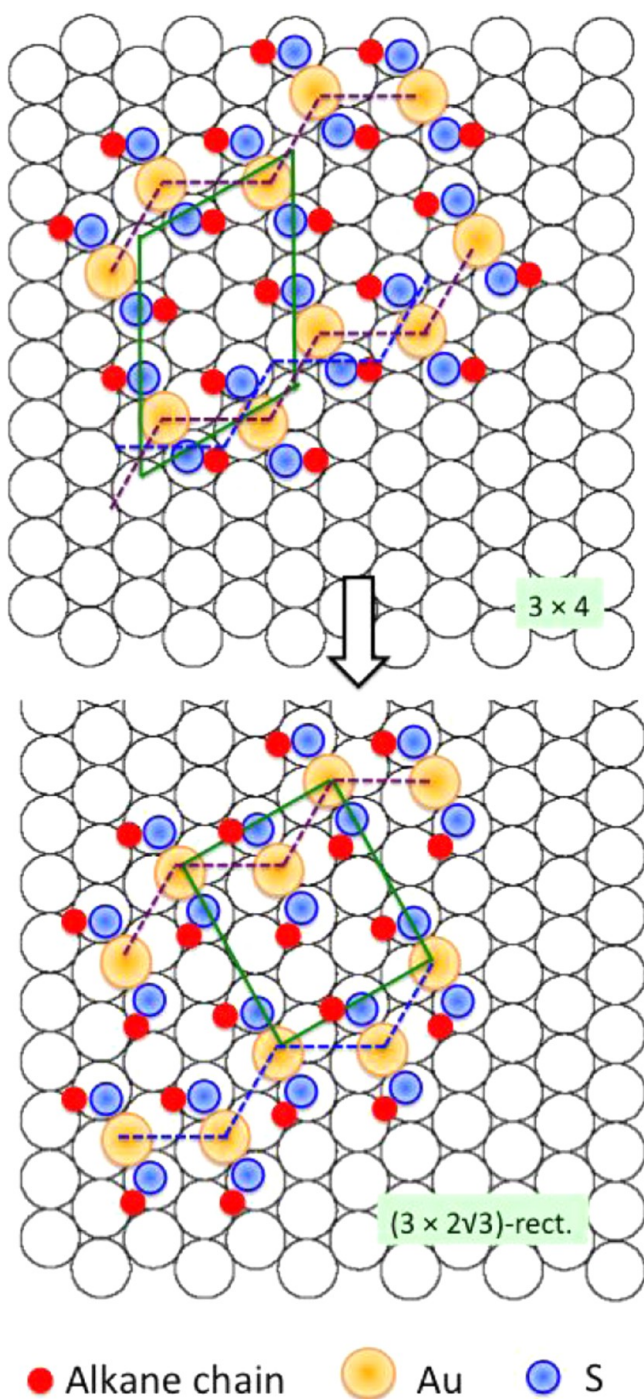
Figure 4. The proposed relationship between the (3×4) and $(3 \times 2\sqrt{3})$-rect./$c(4 \times 2)$ phases. Both phases consist of zig-zag rows of AAD. For (3×4), all AAD rows follow the same zig-zag sequence. For $(3 \times 2\sqrt{3})$-rect./$c(4 \times 2)$, AAD rows take an alternating zig-zag and zag-zig arrangement. There is also a *trans−cis* isomerization change for the individual AAD when moving from (3×4) to $(3 \times 2\sqrt{3})$-rect./$c(4 \times 2)$.

According to the model for the $(3 \times 2\sqrt{3})$-rect. phase in Figure 4, the two alkane chains from each AAD have different local co-ordinations with one of them next to the Au adatom of the neighboring AAD. Therefore, half of the alkane chains in the $(3 \times 2\sqrt{3})$-rect. monolayer are expected to be different from the other half, e.g., with different geometric heights. This would automatically lead to the contrast pattern such as that

seen for the δ phase in STM.[12] As the alkane chain length increases further, the influence from the interface on the packing of the methyl groups at the top surface will fade. Eventually, the methyl groups will appear to have a $(\sqrt{3} \times \sqrt{3})$-R30°-like structure. If a depth-profiling X-ray diffraction experiment is conducted, one expects to see a gradual shift from a $(3 \times 2\sqrt{3})$-rect./$c(4 \times 2)$ phase at the interface to a $(\sqrt{3} \times \sqrt{3})$-R30°-like phase at the surface. The interaction between the tails of the thiolates depends not only on the length of the tail but also on the structure of the tail. For example, in an earlier investigation, Poirier et al. found that the mercaptohexanol monolayer formed the (3×4) phase.[53] In their paper, the unit cell was assigned to an alternative oblique cell with dimensions $3a$ and $\sqrt{13}\ a$. It is thus interesting that hydroxyl-functionalized hexanethiol takes the (3×4) phase while hexanethiol monolayer takes the $(3 \times 2\sqrt{3})$-rect./$c(4 \times 2)$ phase. It is likely that the hydrogen bond between the hydroxyl groups helps to stabilize the (3×4) phase. For the high coverage phase of alkanethiol monolayers, direct experimental identification of the AAD is usually difficult. However, the AAD species has been observed for butylthiolate monolayers at less than saturation coverage.[54] Therefore, the scheme presented in Figure 4 could serve as a basis for a universal structural model for alkanethiol SAMs in general.

In terms of theoretical investigations, the complexity of alkanethiol SAMs presents a great challenge. Many of the early studies chose to ignore the dispersive interactions between the alkane chains, resulting in significant uncertainties. Recently, a number of calculations have incorporated the van der Waals interaction[48,55] and demonstrated chain length dependent effects.[48] However, there still lacks a complete agreement between theory and experiments with some theoretical analysis still predicting the $(3 \times 2\sqrt{3})$-rect./$c(4 \times 2)$ phase for MT and ET monolayers.[25,55] The most recent calculations performed by Carro et al.[48] confirm our earlier experimental finding that the (3×4) is the stable structure for MT and ET monolayers. Their calculation predicts the transition from (3×4) to $(3 \times 2\sqrt{3})$-rect./$c(4 \times 2)$ should occur for PT monolayers, while our results show that this transition does not occur until butylthiolate monolayers. Recently, we have also investigated a mixed methyl- and propyl-thiolate monolayer and found the same (3×4) phase.[56] Moreover, an intermediate di-Au-adatom-trithiolate species has been identified during the assembly of ethyl-thiolate monolayers at elevated temperatures, providing additional new insight into the assembly mechanism.[19]

■ CONCLUSIONS

To summarize, for self-assembled monolayers of alkanethiols on Au(111), the chemical bonding between S and Au at the interface forms the initial anchoring points for the molecules and it favors the formation of the (3×4) phase at 1/3 ML coverage. As the alkane chain increases in length, the nonspecific interaction between the chains can shift the anchoring points on the surface, leading to a gross structural change. This type of competition between chemical bonding and van der Waals forces is expected to be rather general in self-assembled systems. The emerging new insights into the structural aspects of alkanethiol SAMs are important in many fields where SAMs are utilized as a functional layer for a range of technological applications.[57]

24988

dx.doi.org/10.1021/jp410738e | J. Phys. Chem. C 2013, 117, 24985−24990

■ AUTHOR INFORMATION

Corresponding Author

*E-mail: Q.Guo@bham.ac.uk. Phone: +44 1214144657. Fax: +44 1214147327.

Present Address

†Department of Physics, Tsinghua University, Beijing, 100084, China.

Notes

The authors declare no competing financial interest.

■ REFERENCES

(1) Love, J. C.; Estroff, L. A.; Kriebel, J. K.; Nuzzo, R. G.; Whitesides, G. M. Self-Assembled Monolayers of Thiolates on Metals as a Form of Nanotechnology. *Chem. Rev.* **2005**, *105*, 1103−1169.

(2) Kind, M.; Wöll, Ch. Organic Surfaces Exposed by Self-Assembled Organothiol Monolayers: Preparation, Characterization, and Application. *Prog. Surf. Sci.* **2009**, *84*, 230−278.

(3) Schreiber, F. Structure and Growth of Self-Assembled Monolayers. *Prog. Surf. Sci.* **2000**, *65*, 151−256.

(4) Maksymovych, P.; Voznyy, O.; Dougherty, D. B.; Sorescu, D. V.; Yates, J. T., Jr. Gold Adatom as a Key Structural Component in Self-Assembled Monolayers of Organosulfur Molecules on Au(111). *Prog. Surf. Sci.* **2010**, *85*, 206−240.

(5) Vericat, C.; Vela, M. E.; Benitez, G.; Carro, P.; Salvarezza, R. C. Self-Assembled Monolayers of Thiols and Dithiols on Gold: New Challenges for a Well-known System. *Chem. Soc. Rev.* **2010**, *39*, 1805−1834.

(6) Han, P.; Kurland, A. R.; Giordano, A. N.; Nanayakkara, S. U.; Blake, M. M.; Pochas, C. M.; Weiss, P. S. Heads and Tails: Simultaneous Exposed and Buried Interface Imaging of Monolayers. *ACS Nano* **2009**, *3*, 3115−3121.

(7) Woodruff, D. P. The Role of Reconstruction in Self-Assembly of Alkylthiolate Monolayers on Coinage Metal Surfaces. *Appl. Surf. Sci.* **2007**, *254*, 76−81.

(8) Yang, G.-H.; Liu, G.-Y. New Insights for Self-Assembled Monolayers of Organothiols on Au(111) Revealed by Scanning Tunneling Microscopy. *J. Phys. Chem. B* **2003**, *107*, 8746−8759.

(9) Poirier, G. E.; Pylant, E. D. The Self-Assembly Mechanism of Alkanethiols on Au(111). *Science* **1996**, *272*, 1145−1148.

(10) Toerker, M.; Staub, R.; Fritz, T.; Schmitz-Hubsch, T.; Sellam, F.; Leo, K. Annealed Decanethiol Monolayers on Au(111) - Intermediate Phases Between Structures with High and Low Molecular Surface Density. *Surf. Sci.* **2000**, *445*, 100−108.

(11) Sharma, M.; Komiyama, M.; Engstrom, J. R. Observation from Scanning Tunneling Microscopy of a Striped Phase for Octanethiol Adsorbed on Au(111) from Solution. *Langmuir* **2008**, *24*, 9937−9940.

(12) Lussem, B.; Muller-Meskamp, L.; Karthauser, S.; Waser, R. A New Phase of the c(4 × 2) Superstructure of Alkanethiols Grown by Vapour Phase Deposition on Gold. *Langmuir* **2005**, *21*, 5256−5258.

(13) Teran, F.; Vela, M. E.; Salvarezza, R. C.; Arvia, A. J. The Dynamic Behavior of Butanethiol and Dodecanethiol Adsorbates on Au(111) Terraces. *J. Chem. Phys.* **1998**, *109*, 5703−5706.

(14) Xiao, X.; Wang, B.; Zhang, C.; Yang, Z.; Loy, M. M. T. Thermal Annealing Effect of Alkanethiol Monolayers on Au(111) in Air. *Surf. Sci.* **2001**, *472*, 41−50.

(15) Guo, Q.; Sun, X.; Palmer, R. E. Structural Dynamics Induced by Self-Assembled Monolayers on Au(111). *Phys. Rev. B* **2005**, *71*, 035406.

(16) Keel, J. M.; Yin, J.; Guo, Q.; Palmer, R. E. Layer by Layer Removal of Au Atoms from Passivated Au(111) Surfaces Using STM: Nanoscale "Paint Stripping". *J. Chem. Phys.* **2002**, *116*, 7151−7157.

(17) Li, F. S.; Tang, L.; Zhou, W.-C.; Guo, Q. Adsorption Site Determination for Au-Octanethiolate on Au(111). *Langmuir* **2010**, *26*, 9484−9490.

(18) Li, F. S.; Tang, L.; Zhou, W.-C.; Guo, Q. Resolving the Au-Adatom-Alkanethiolate Bonding Site on Au(111) with Domain Boundary Imaging using High-Resolution Scanning Tunneling Microscopy. *J. Am. Chem. Soc.* **2010**, *132*, 13059−13063.

(19) Li, F. S.; Tang, L.; Voznyy, O.; Gao, J.; Guo, Q. The Striped Phases of Ethylthiolate Monolayers on the Au(111) Surface: A Scanning Tunneling Microscopy Study. *J. Chem. Phys.* **2013**, *138*, 194707−194713.

(20) Li, F. S.; Tang, L.; Zhou, W.-C.; Guo, Q. Relationship Between the c(4 × 2) and the ($\sqrt{3} \times \sqrt{3}$)R30° Phases in Alkanethiol Self-Assembled Monolayers on Au(111). *Phys. Chem. Chem. Phys.* **2011**, *13*, 11958−11964.

(21) Li, F. S.; Zhou, W.-C.; Guo, Q. Uncovering the Hidden Gold Atoms in a Self-Assembled Monolayer of Alkanethiol Molecules on Au(111). *Phys. Rev. B* **2009**, *79*, 113412.

(22) Dubois, L. H.; Zegarski, B. R.; Nuzzo, R. G. Molecular Ordering of Organosulfur Compounds on Au(111) and Au(100)- Adsorption from Solution and in Ultra-high Vacuum. *J. Chem. Phys.* **1993**, *98*, 678−688.

(23) Camillone, N., III; Eissenberger, P.; Leung, T. Y. B.; Schwartz, P.; Scoles, G.; Poirier, G. E.; Tarlov, M. J. New Monolayer Phases of n-alkane Thiols Self-Assembled on Au(111)-Preparation, Surface Characterization, and Imaging. *J. Chem. Phys.* **1994**, *101*, 11031−11036.

(24) Pflaum, J.; Bracco, G.; Schreiber, F.; Colorado, R.; Shmakova, O. E.; Lee, T. R.; Scoles, G.; Kahn, A. Structure and Electronic Properties of CH₃ - and CF₃−Terminated Alkanethiol Monolayers on Au(111): A Scanning Tunneling Microscopy, Surface x-ray and Helium Scattering Study. *Surf. Sci.* **2002**, *498*, 89−104.

(25) Ishida, T.; Hara, M.; Kojima, I.; Tsuneda, S.; Nishida, N.; Sasabe, H.; Knoll, W. High Resolution x-ray Photoelectron Spectroscopy Measurements of Octadecanethiol Self-Assembled Monolayers on Au(111). *Langmuir* **1998**, *14*, 2092−2096.

(26) Noh, J.; Kato, H.; Kawai, M.; Hara, M. Surface Structure and Interface Dynamics of Alkanethiol Self-Assembled Monolayers on Au(111). *J. Phys. Chem. B* **2006**, *110*, 2793−2797.

(27) Torrelles, X.; Barrena, E.; Unuera, C.; Rius, J.; Ferrer, S.; Ocal, C. New Insights in the c(4 × 2) Reconstruction of Hexadecanethiol on Au(111) Revealed by Grazing Incidence x-ray Diffraction. *Langmuir* **2004**, *20*, 9396−9402.

(28) Fenter, P.; Eisenberger, P.; Liang, K. S. Chain-length Dependence of the Structures and Phases of CH₃(CH₂)ₙ-SH Self-Assembled on Au(111). *Phys. Rev. Lett.* **1993**, *70*, 2447−2450.

(29) Strong, L.; Whitesides, G. M. Structures of Self-assembled Monolayer Films of Organosulfur Compounds Adsorbed on Gold Single Crystals: Electron Diffraction Studies. *Langmuir* **1988**, *14*, 546−558.

(30) Camillone, N.; Chidsey, C. E. D.; Liu, G. Y.; Scoles. Superlattice Structure at the Surface of a Monolayer of Octadecanethiol Self-assembled on Au(111). G. *J. Chem. Phys.* **1993**, *98*, 3503−3511.

(31) Kondoh, H.; Iwasaki, M.; Shimada, T.; Amemiya, K.; Yokoyama, T.; Ohta, T.; Shimomura, M.; Kono, S. Adsorption of Thiolates to Singly Coordinated Sites on Au(111) Evidenced by Photoelectron Diffraction. *Phys. Rev. Lett.* **2003**, *90*, 066102.

(32) Roper, M. G.; Skegg, M. P.; Fisher, C. J.; Lee, J. J.; Dhanak, V. R.; Woodruff, D. P.; Jones, R. G. Atop Adsorption Site of Sulphur Head Groups in Gold-thiolate Self-assembled Monolayers. *Chem. Phys. Lett.* **2004**, *389*, 87−91.

(33) Picraux, L. B.; Zangmeister, C. D.; Batteas, J. D. Preparation and Structure of a Low-Density, Flat-lying Decanethiol Monolayer from the Densely Packed, Upright Monolayer on Gold. *Langmuir* **2006**, *22*, 174−180.

(34) Chailapakul, O.; Sun, L.; Xu, C. J.; Crooks, R. M. Interactions Between Organized, Surface-confined Monolayers and Vapor-phase Probe Molecules: Comparison of Self-Assembled *n*-alkanethiol

Monolayers Deposited on Gold from Liquid and Vapor Phases. *J. Am. Chem. Soc.* **1993**, *115*, 12459–12467.

(35) Nishida, N.; Hara, M.; Sasabe, H.; Knoll, W. Formation and Exchange Processes of Alkanethiol Self-assembled Monolayer on Au(111) Studied by Thermal Desorption Spectroscopy and Scanning Tunneling Microscopy. *Jpn. J. Appl. Phys.* **1997**, *36*, 2379–2385.

(36) Yu, M.; Bovet, N.; Satterley, C. J.; Bengio, S.; Lovelock, K. R. J.; Milligan, P. K.; Jones, R. G.; Woodruff, D. P.; Dhanak, V. True Nature of an Archetypal Self-Assembly System: Mobile Au-Thiolate Species on Au(111). *Phys. Rev. Lett.* **2006**, *97*, 166102–166105.

(37) Kautz, N. A.; Kandel, S. A. Alkanethiol/Au(111) Self-Assembled Monolayers Contain Gold Adatoms: Scanning Tunneling Microscopy Before and After Reaction with Atomic Hydrogen. *J. Am. Chem. Soc.* **2008**, *130*, 6908–6909.

(38) Voznyy, O.; Dubowski, J. J.; Yates, J. T., Jr.; Maksymovych, P. The Role of Gold Adatoms and Stereochemistry in Self-Assembly of Methylthiolate on Au(111). *J. Am. Chem. Soc.* **2009**, *131*, 12989–12993.

(39) Gronbeck, H.; Hakkinen, H.; Whetten, R. L. Gold−Thiolate Complexes Form a Unique c(4 × 2) Structure on Au(111). *J. Phys. Chem. C* **2008**, *112*, 15940–15942.

(40) Mazzarello, R.; Cossaro, A.; Verdini, A.; Rousseau, R.; Casalis, L.; Danisman, M. F.; Floreano, L.; Scandolo, S.; Morgante, A.; Scoles, G. Structure of a CH$_3$S Monolayer on Au(111) Solved by the Interplay Between Molecular Dynamics Calculations and Diffraction Measurements. *Phys. Rev. Lett.* **2007**, *98*, 016102.

(41) Chaudhuri, A.; Lerotholi, T. J.; Jackson, D. C.; Woodruff, D. P. (2√3 × 3)-rect. Phase of Alkylthiolate Self-Assembled Monolayers on Au(111): A Symmetry-Constrained Structural Solution. *Phys. Rev. B* **2009**, *79*, 195439.

(42) Wang, Y.; Chi, Q.; Hush, N. S.; Remers, J. R.; Zhang, J.-D.; Ulstrup, J. Gold Mining by Alkanethiol Radicals: Vacancies and Pits in the Self-assembled Monolayers of 1-propanethiol and 1-butanethiol on Au(111). *J. Phys. Chem. C* **2011**, *115*, 10630–10639.

(43) Chesneau, F.; Zhao, J.; Shen, C.; Buck, M.; Zharnikov, M. Adsorption of Long-Chain Alkanethiols on Au(111) - a Look from the Substrate by High Resolution X-ray Photoelectron Spectroscopy. *J. Phys. Chem. C* **2010**, *114*, 7112–7119.

(44) Jiang, D.-E.; Dai, S. Cis−trans Conversion of the CH$_3$S−Au−SCH$_3$ Complex on Au(111). *Phys. Chem. Chem. Phys.* **2009**, *11*, 8601–8605.

(45) Liu, Y.; Ozolins, V. Self-Assembled Monolayers on Au(111): Structure, Energetics, and Mechanism of Reconstruction Lifting. *J. Phys. Chem. C* **2012**, *116*, 4738–4747.

(46) Tang, L.; Li, F. S.; Zhou, W.-C.; Guo, Q. The Structure of Methylthiolate and Ethylthiolate Monolayers on Au(111): Absence of the (√3 × √3)R30° Phase. *Surf. Sci.* **2012**, *606*, L31–L35.

(47) Clair, S.; Kim, Y.; Kawai, M. Coverage-Dependent Formation of Chiral Ethylthiolate-Au Complexes on Au(111). *Langmuir* **2011**, *27*, 627–629.

(48) Carro, P.; Pensa, E.; Vericat, C.; Salvarezza, R. C. Hydrocarbon Chain Length Induces Surface Structure Transitions in Alkanethiolate-Gold Adatom Self-Assembled Monolayers on Au(111). *J. Phys. Chem. C* **2013**, *117*, 2160–2165.

(49) Maksymovych, P.; Sorescu, D. C.; Voznny, O.; Yates, J. T., Jr. Hybridization of Phenylthiolate- and Methylthiolate-adatom Species at Low Coverage on the Au(111) Surface. *J. Am. Chem. Soc.* **2013**, *135*, 4922–4925.

(50) Hakkinen, H. The Gold-Sulfur Interface at the Nanoscale. *Nat. Chem.* **2012**, *4*, 443–455.

(51) Tang, L.; Li, F. S.; Guo, Q. Complete Structural Phases for Self-Assembled Methylthiolate Monolayers on Au(111). *J. Phys. Chem. C* **2013**, *117*, 21234.

(52) Palmer, R. E.; Robinson, A. P. G.; Guo, Q. How Nanoscience Translates into Technology: The Case of Self-Assembled Monolayers, Electron-Beam Writing, and Carbon Nanomembranes. *ACS Nano* **2013**, *7*, 6416–6421.

(53) Poirier, G. E.; Pylant, E. D.; White, J. M. Crystalline Structure of Pristine and Hydrated Mercaptohexanol Self-Assembled Monolayers on Au(111). *J. Chem. Phys.* **1996**, *105*, 2089–2092.

(54) Chaudhuri, A.; Jackson, D. C.; Lerotholi, T. J.; Jones, R. G.; Lee, T. L.; Detlefs, B.; Woodruff, D. P. Structure Investigation of Au(111)/Butylthiolate Adsorption Phases. *Phys. Chem. Chem. Phys.* **2010**, *12*, 3229–3238.

(55) Ferrighi, L.; Pan, Y.-X.; Gronbeck, H.; Hammer, B. Study of Alkylthiolate Self-Assembled Monolayers on Au(111) Using a Semi-Local Meta-GGA Density Functional. *J. Phys. Chem. C* **2012**, *116*, 7374–7379.

(56) Li, F. S.; Gao, J.; Guo, Q. Mixed Methyl- and Propylthiolate Monolayers on the Au(111) Surface. *Langmuir* **2013**, *29*, 11082–11086.

(57) Azcarate, J. C.; Corthey, G.; Pensa, E.; Vericat, C.; Fonticelli, M. H.; Salvarezza, R. C.; Carro, P. Understanding the Surface Chemistry of Thiolate-Protected Metallic Nanoparticles. *J. Phys. Chem. Lett.* **2013**, *4*, 3127–3138.